Electronic Supplementary Material (ESI) for Materials Chemistry Frontiers.
This journal is © the Partner Organisations 2020

Electronic Supplementary Information

An off-the-shelf microfluidic device for the controllable fabrication of multiple-holed hollow particles and their cell culture application

Lili Sun, Tianbao Li,* Baojin Zhang, Meng Zhang, Juan Xu and Jinyi Wang*

College of Chemistry & Pharmacy, Northwest A&F University, Yangling, Shaanxi 712100, China

**Corresponding authors*
E-mail: litianbao@nwsuaf.edu.cn
jywang@nwsuaf.edu.cn

This document includes:

Experimental details: S1. Materials and Chemicals; S2. Cell Preparation; S3. Cell Staining; S4. Characterization.

Figures: S1; S2; S3; S4; S5; S6; S7; S8; S9; S10; S11; S12; S13; S14; S15.

Movies: S1; S2; S3; S4.

EXPERIMENTAL DETAILS

S1. Materials and Chemicals

Poly(vinyl alcohol) (PVA, Mw 13000–23000), ethoxylated trimethylolpropane triacrylate (ETPTA, Mw 428), ethylene oxide–propylene oxide–ethylene oxide triblock copolymer surfactant (Pluronic F108), octadecyl trichlorosilane (OTS), and 2-hydroxy-2-methylpropiophenone (HMPP) were obtained from Sigma-Aldrich (Shanghai, China). Fe_3O_4 nanoparticles (smaller than 50 nm) were purchased from Aladdin Chemistry Co., Ltd. UV curing adhesive (Kafuter K-302), UV-LED light (365 nm, 30 W), dispensing needles, glass capillaries, cross-connects, and tee-connects were obtained through the Alibaba website. All solutions were prepared using ultra-purified water (Millipore®).

S2. Cell Preparation

Human hepatocellular liver carcinoma (HepG2) were obtained from the Chinese Academy of Sciences (Shanghai, China). The cells were cultured under a humidified atmosphere (5% CO_2) at 37 °C. The culture medium was DMEM supplemented with 10% (v/v) FBS, 100 μg mL^{-1} streptomycin, and 100 units' mL^{-1} penicillin. Cells were passaged every 3 days (ratio of 1 : 3) to maintain their exponential growth phase. Before use, cells were harvested by trypsinization with 0.25% trypsin-EDTA at 37 °C for 5 min and stopped by adding fresh DMEM. The cell suspension was centrifuged (3 min, 800 rpm) and then resuspended in supplemented DMEM for use.

S3. Cell Staining

Cell viability within the 3D tumor spheroids was evaluated using FDA/PI staining protocol. After removing the medium from the cells and rinsing with PBS, the FDA/PI (10 μg mL^{-1} each in PBS) staining solution was added to the petri dish, and the staining process was performed for 15 min at 37 °C. The cells were then washed with PBS to remove the extra fluorescent dyes

before being imaged. During these procedures, the dead cells were stained red by the fluorescent dye PI, whereas the living cells were stained green by the fluorescent dye FDA. For quantitative analysis of chemotherapy, the percentage of cell death in the 3D tumor spheroids was calculated by the formula: $100 \times (1\text{-}A_d/A_t)$, where A_d is the area of dead cells in and A_t is the total area of the tumor spheroids.

S4. Characterization

The formation of emulsion droplets was monitored by an inverted optical microscope (Olympus, DP73). The images of the droplets and the hollow particles were captured by a CCD (Olympus, CKX41) connected to the microscope. The hollow particles' microstructures were further characterized by a scanning electron microscope (SEM, Hitachi, and S-4800).

FIGURES

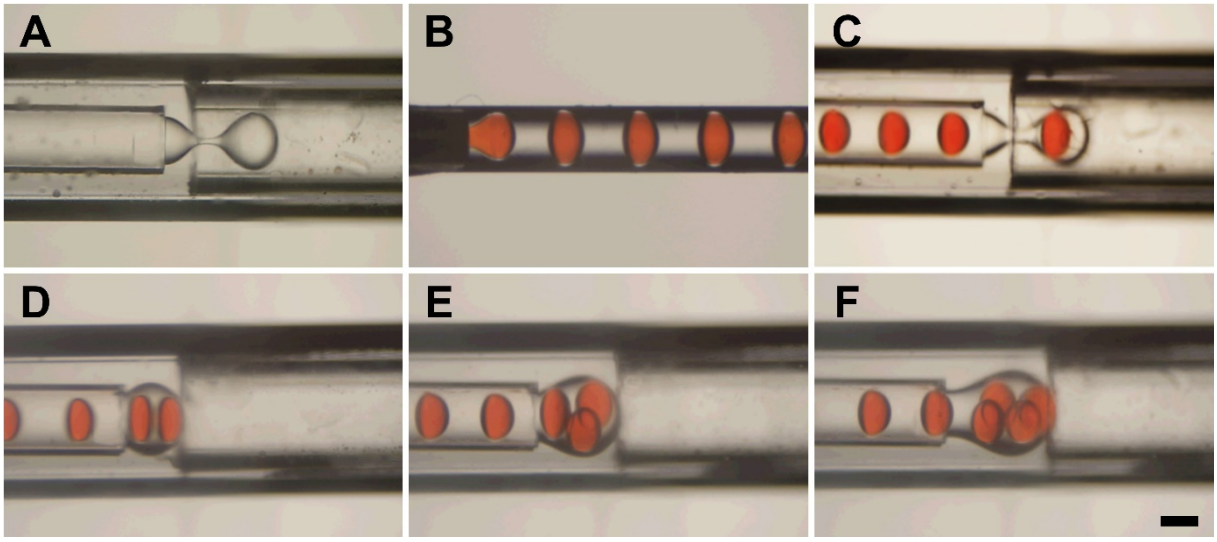

Figure S1. Real-time images of the microfluidic fabrication of multiple-core emulsion droplets by adjusting the distance between two glass capillaries. (A) Single emulsion droplets. (B) Inner core droplets. (C) Double emulsion droplets with one core. (D) Double emulsion droplets with two cores. (E) Double emulsion droplets with three cores. (F) Double emulsion droplets with four cores. The scale bar is 200 μm.

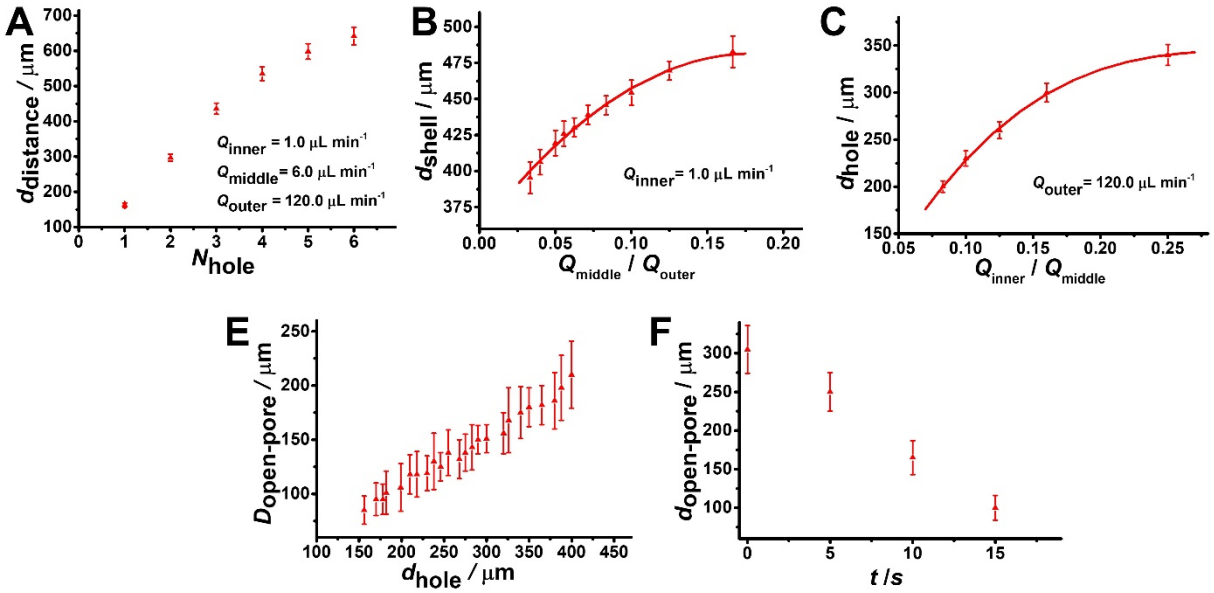

Figure S2. Fabrication condition effects on the hollow particles. (A) Effect of the inter-capillary distance ($d_{distance}$, distance between 300 and 500 μm sized glass capillaries) on the number of the holes (N_{hole}). (B) Shell diameter (d_{shell}) versus the flow rate ratio Q_{middle}/Q_{outer} at fixed $d_{distance}$ (162 μm). (C) Hole diameter (d_{hole}) versus the flow rate ratio Q_{inner}/Q_{middle} at fixed $d_{distance}$ (162 μm). (D) Open-pore diameter ($d_{open-pore}$) versus the hole diameter (d_{hole}). The polymerization was carried after equilibrium of the core droplet was reached. (E) Effect of the UV-polymerization start time (t, the time before equilibration of the core droplet) on the open-pore diameter ($d_{open-pore}$). The obtained particles were the same in diameter of hole and shell (d_{shell} = 651 μm, d_{hole} = 575 μm).

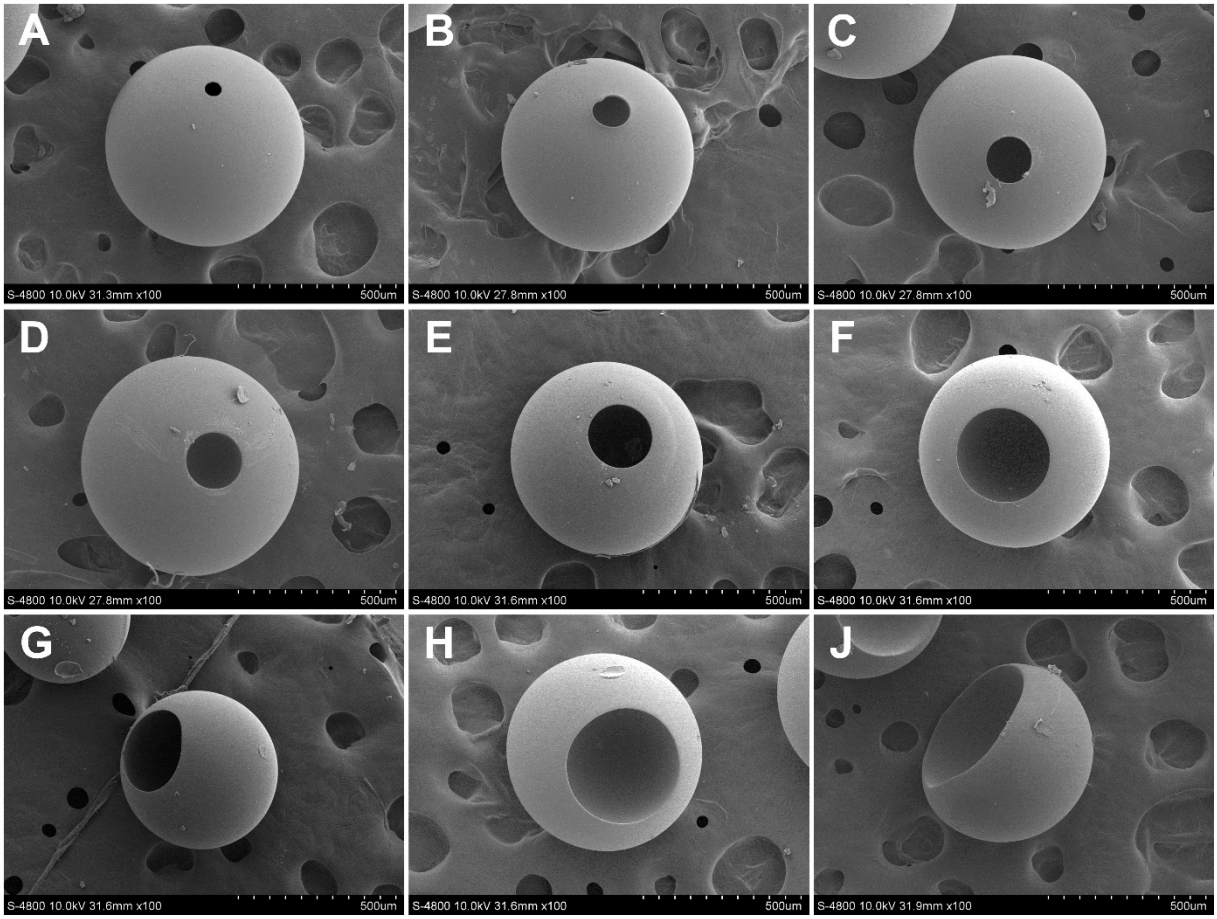

Figure S3. SEM photographs of single-holed hollow particles with different sizes and shapes. The diameters of the open-pore and the hollow particle in A to J are 54/636μm, 122/605μm, 145/610 μm, 173/689 μm, 203/607 μm, 296/673 μm, 269/495 μm, 358/623 μm, and 460/586 μm, respectively.

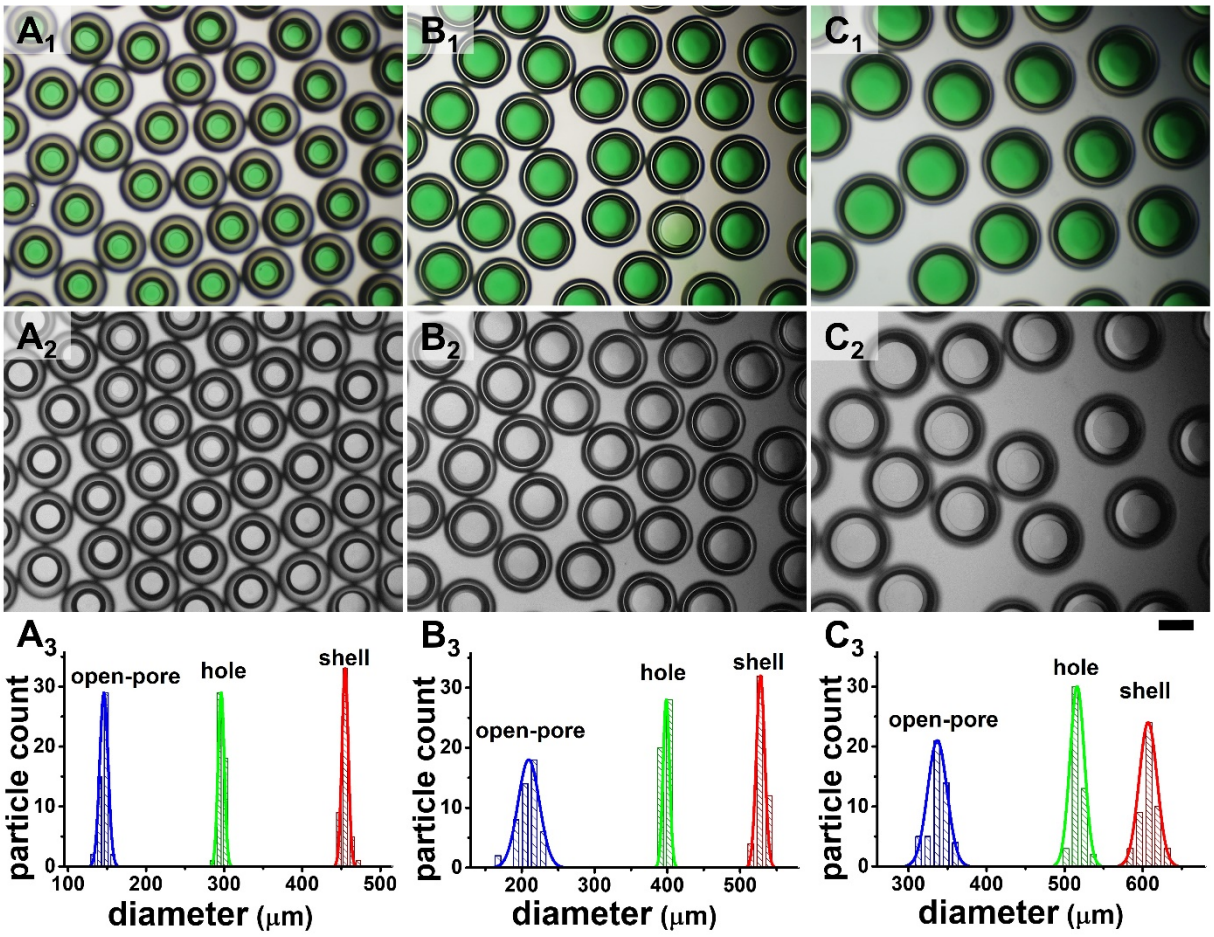

Figure S4. Micrographs of single-holed hollow particles with different sizes and shapes (A_1, A_2, B_1, B_2, C_1, and C_2). The statistical size distribution histograms of the open-pore, hole, and shell (A_3, B_3, and C_3). The scale bar is 300 μm.

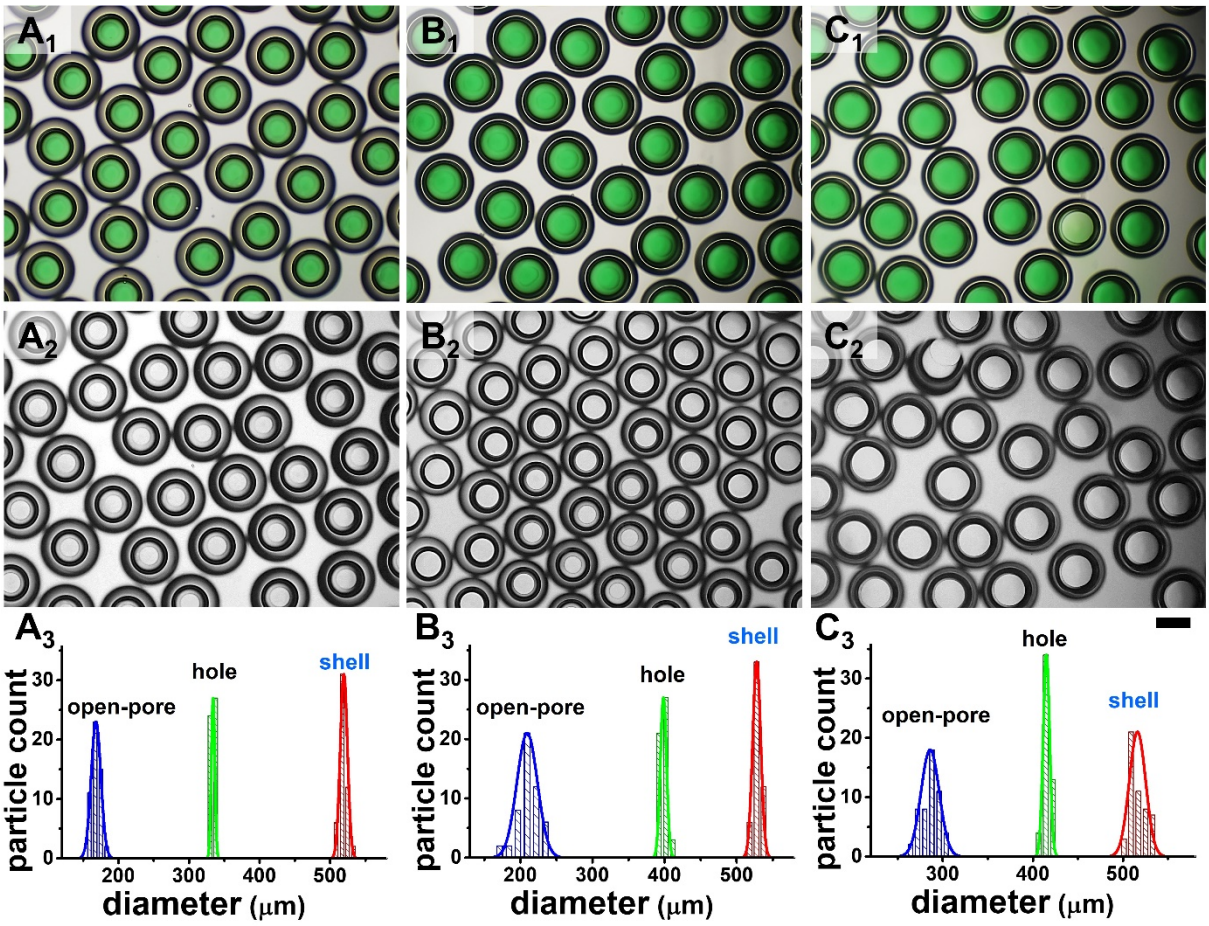

Figure S5. Micrographs of single-holed hollow particles with the same sized shell and different sized hole and open-pore (A_1, A_2, B_1, B_2, C_1, and C_2). The statistical size distribution histograms of the open-pore, hole, and shell (A_3, B_3, and C_3). The scale bar is 300 μm.

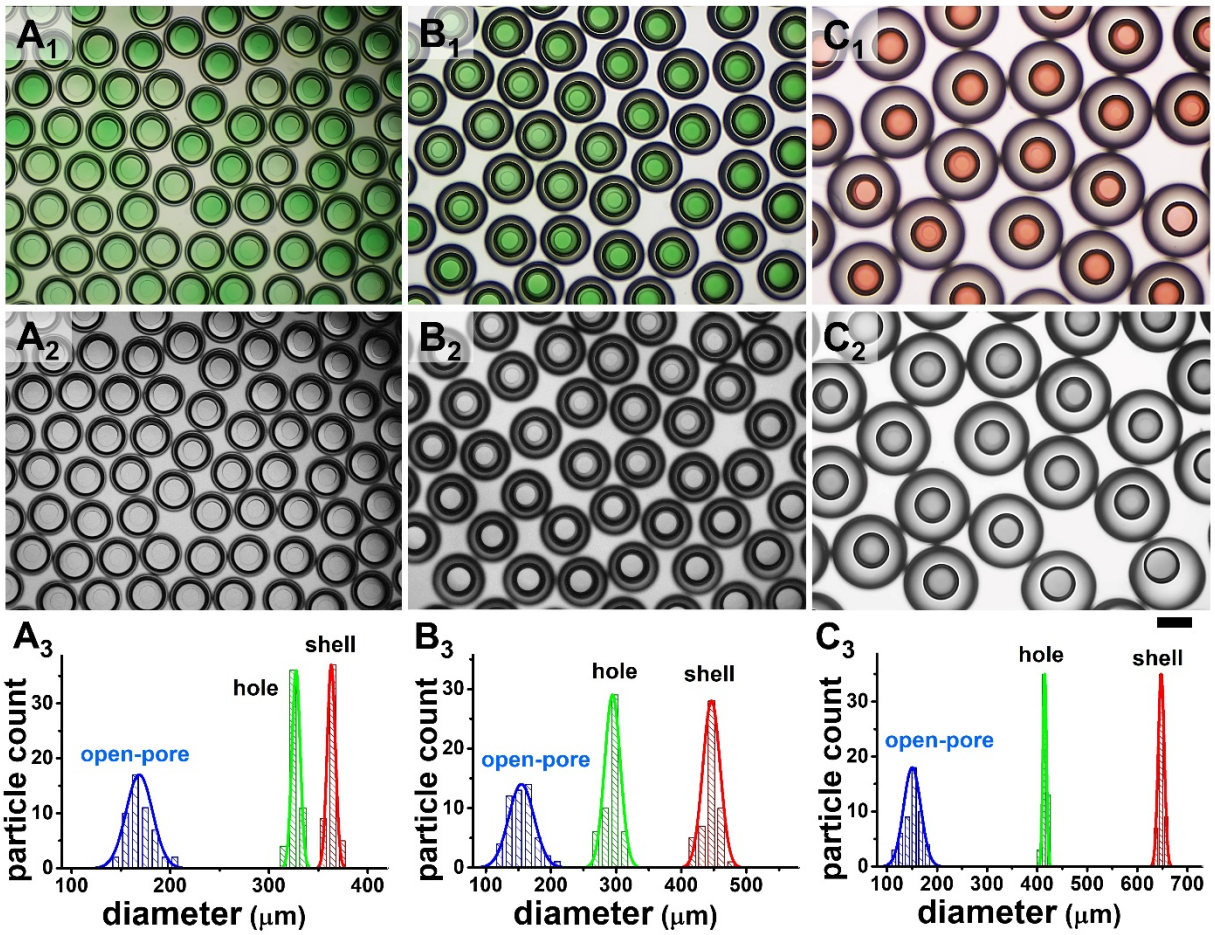

Figure S6. Micrographs of single-holed hollow particles with same sized open-pore and different sized hole and shell (A_1, A_2, B_1, B_2, C_1, and C_2). The statistical size distribution histograms of the open-pore, hole, and shell (A_3, B_3, and C_3). The scale bar is 300 μm.

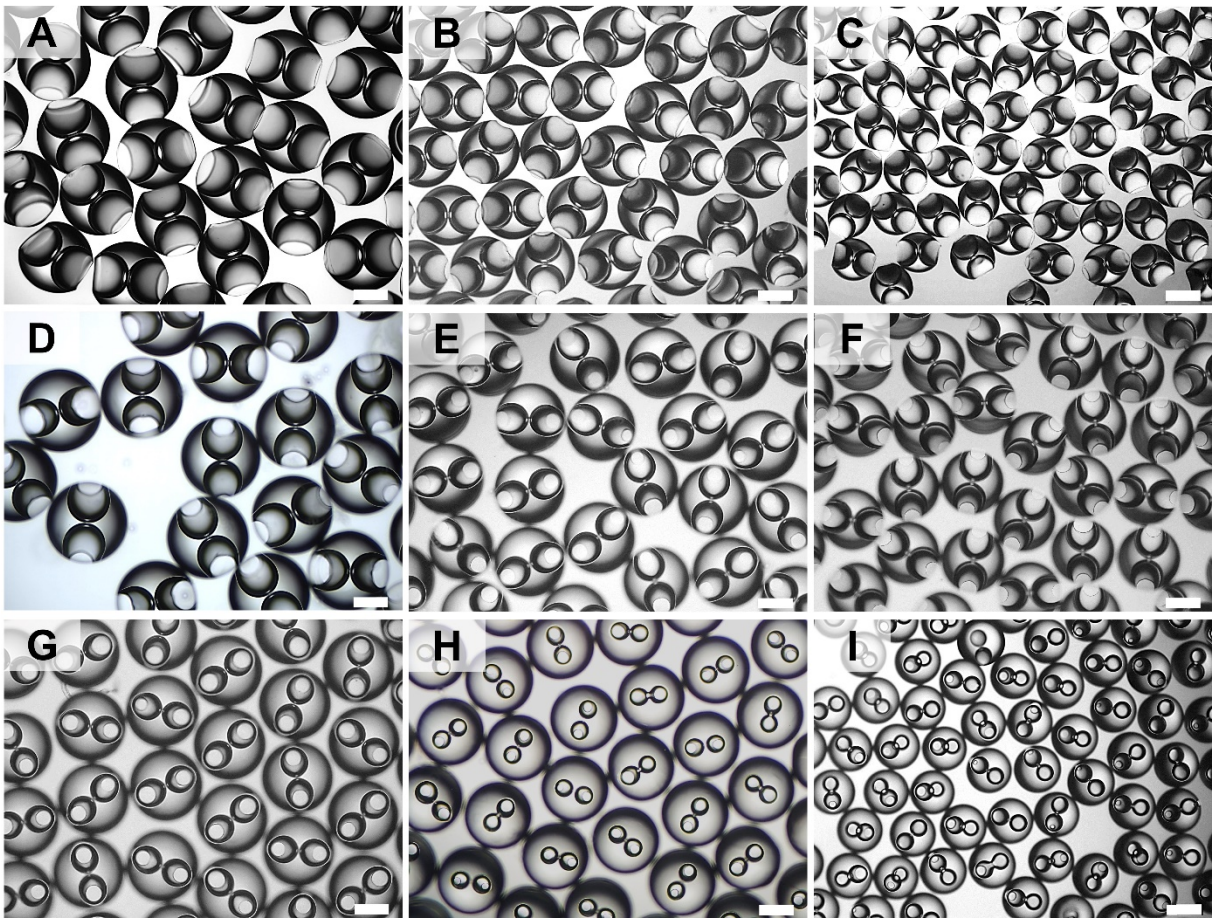

Figure S7. Micrographs of double-holed hollow particles with different sizes and shapes. The diameters of the open-pore and the particle in A to I are 273 ± 26/413 ± 22/636 ± 11 μm, 168 ± 38/316 ± 12/530 ± 8 μm, 148 ± 25/246 ± 10/362 ± 6 μm, 241 ± 26/361 ± 13/699 ± 15 μm, 132 ± 18/268 ± 10/595 ± 16 μm, 143 ± 21/283 ± 15/538 ± 10 μm, 138 ± 13/246 ± 5/613 ± 16 μm, 71 ± 16/148 ± 8/582 ± 9 μm, and 53 ± 21/158 ± 9/398 ± 6 μm, respectively. Scale bars are 300 μm.

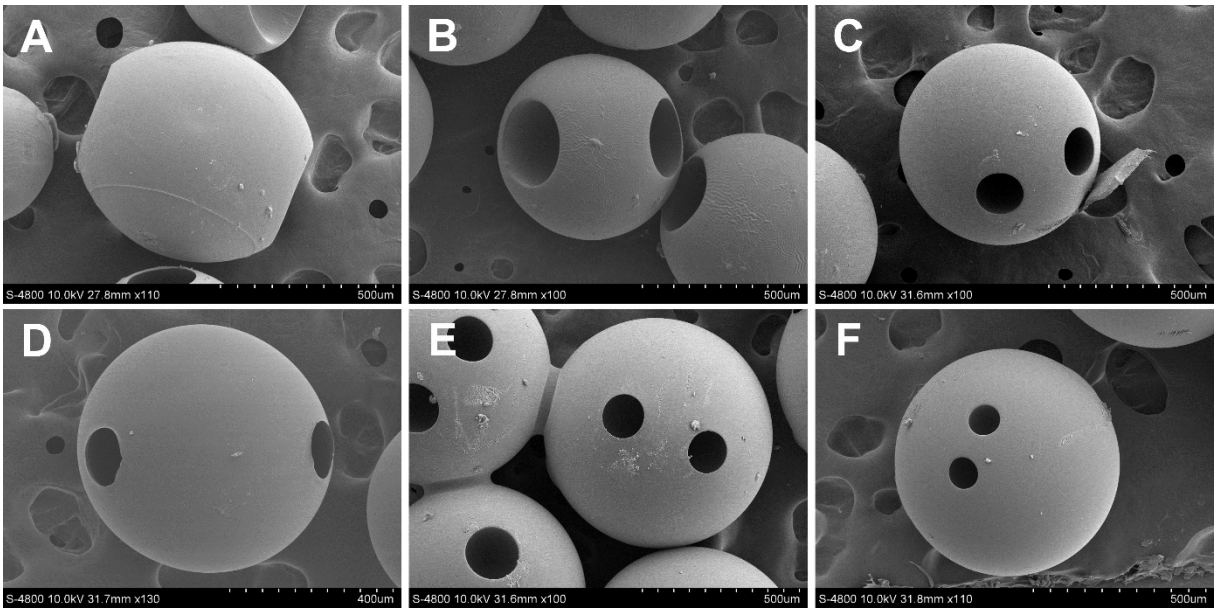

Figure S8. SEM photographs of double-holed hollow particles with different sizes and shapes. The diameters of the open-pore and the hollow particle in A to F are 255/631μm, 275/598μm, 144/641 μm, 141/613 μm, 137/734 μm, and 92/654 μm, respectively.

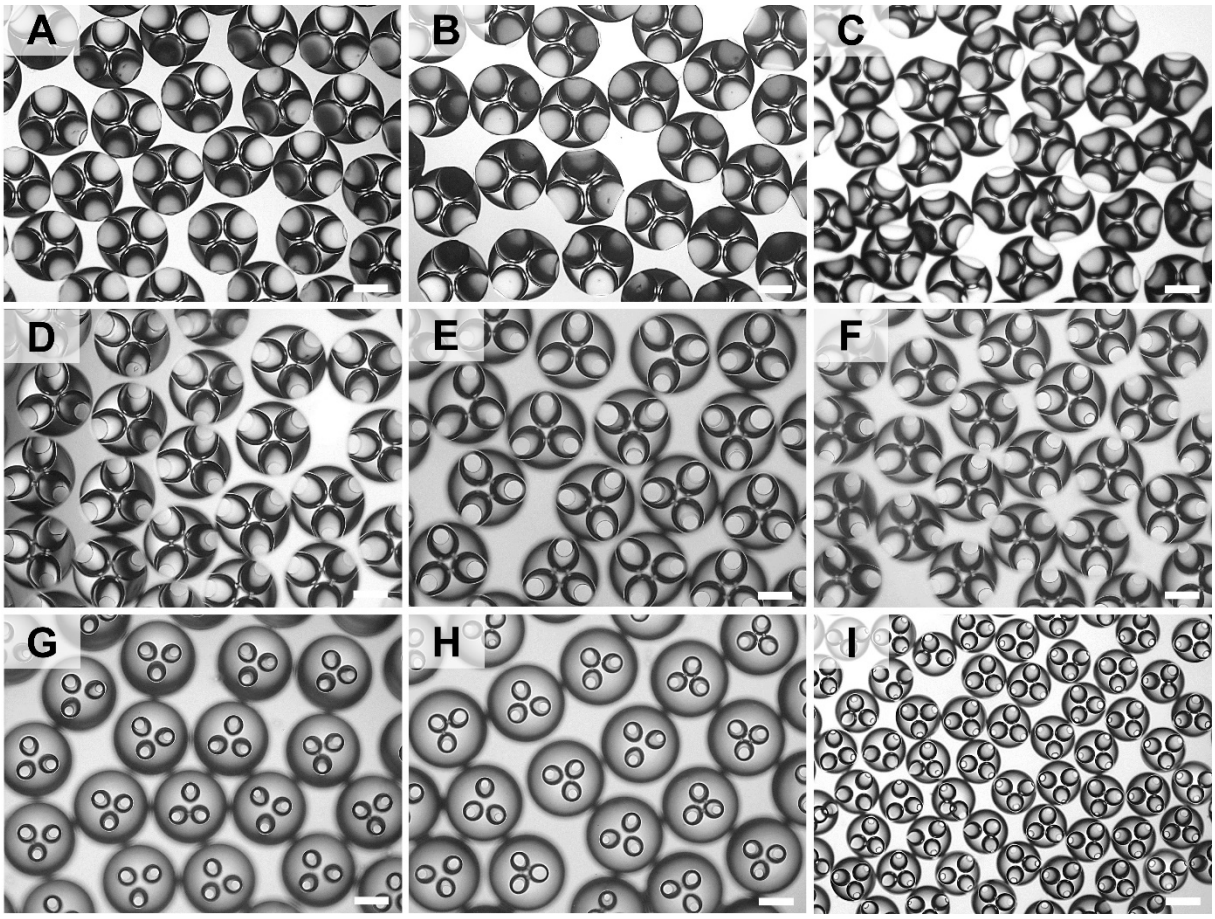

Figure S9. Micrographs of triple-holed hollow particles with different sizes and shapes. The diameters of the open-pore and the particle in A to I are 141 ± 16/325 ± 10/610 ± 6 μm, 180 ± 23/342 ± 25/628 ± 14 μm, 243 ± 14/320 ± 12/570 ± 18, 169 ± 13/291 ± 8/637 ± 11 μm, 150 ± 13/278 ± 8/678 ± 10 μm, 138 ± 17/275 ± 8/593 ± 13 μm, 85 ± 7/156 ± 6/648 ± 9 μm, 71 ± 13/165 ± 7/662 ± 8 μm, and 38 ± 16/150 ± 8/382 ± 6 μm, respectively. The scale bars are 300 μm.

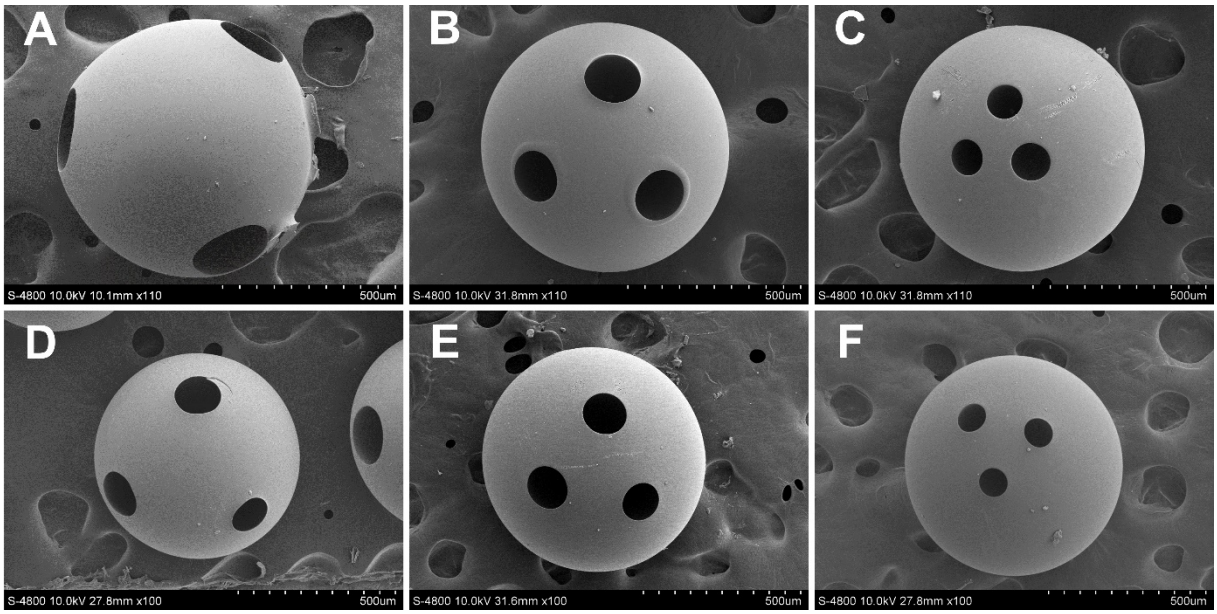

Figure S10. SEM photographs of triple-holed hollow particles with different sizes and shapes. The diameters of the open-pore and the hollow particle in A to F are 243/750 μm, 153/711μm, 120/715 μm, 125/652 μm, 134/709 μm, and 110/697 μm, respectively.

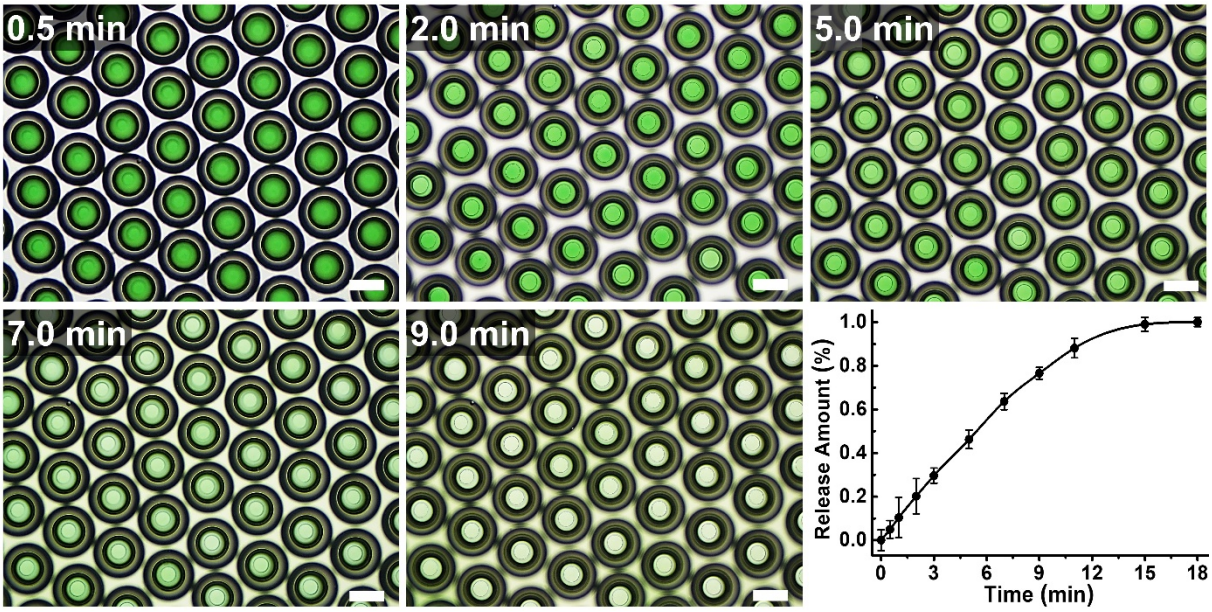

Figure S11. Release of green food coloring from the single-holed hollow particles visualized with micrograph and a graph showing release amount versus time. Scale bars are 300 μm.

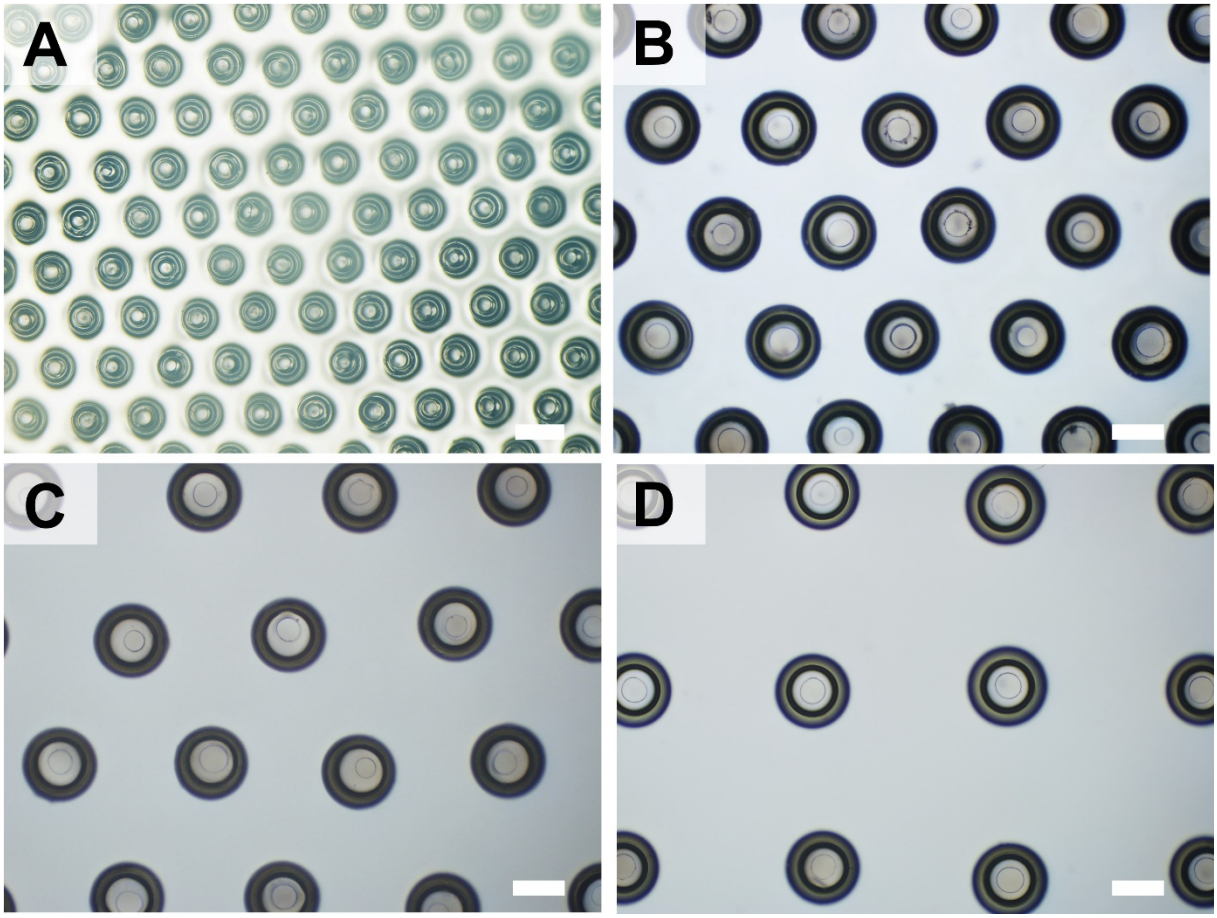

Figure S12. Digital photograph (A) and micrographs (B, C, D) of the prepared single-holed hollow particle arrays with different arrangements. Scale bar in (A) is 500 μm, and others are 300 μm.

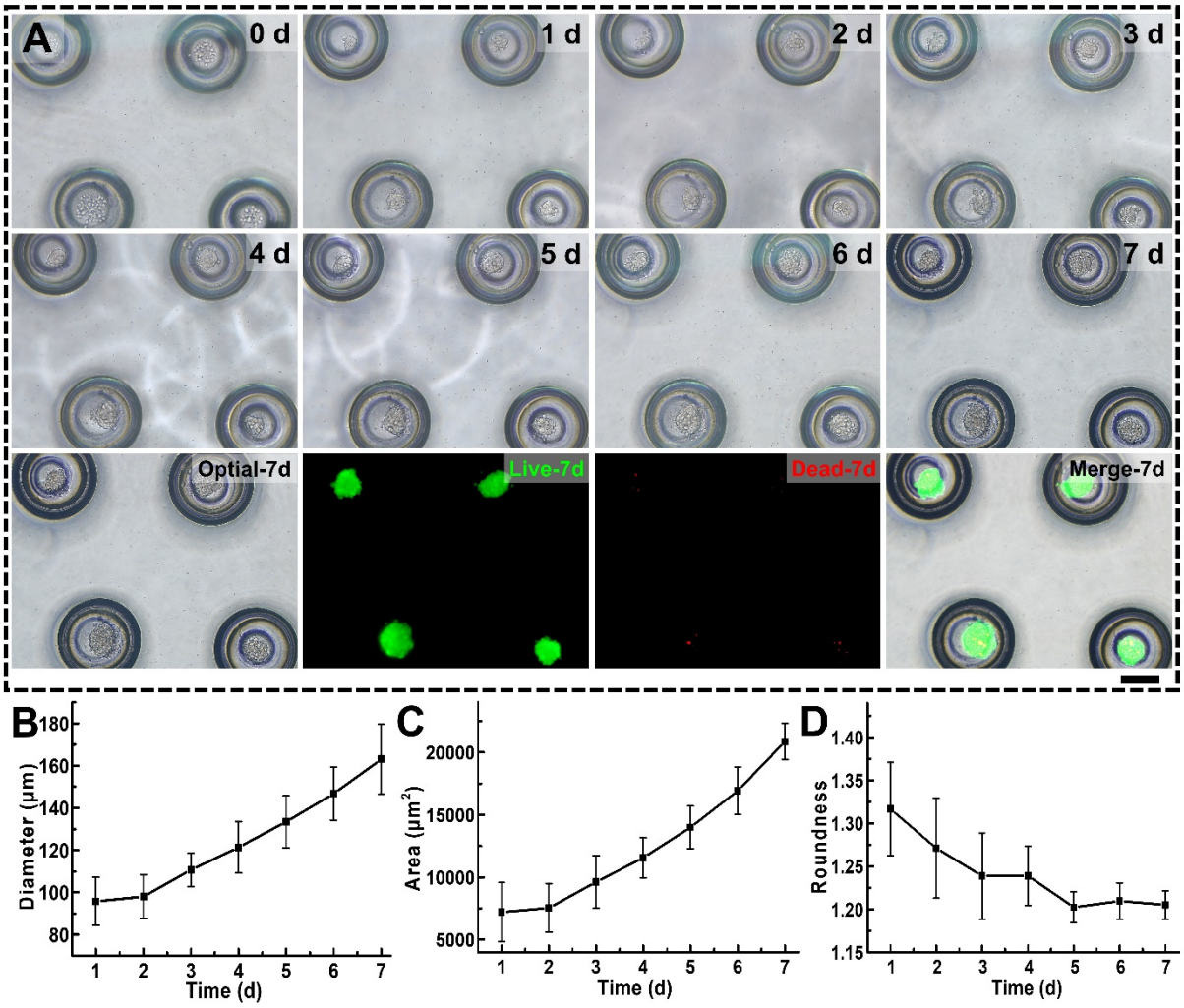

Figure S13. Investigation of 3D tumor spheroids in single-holed hollow particle arrays. (A) Bright-field images and the corresponding FDA/PI co-staining fluorescent images of HepG2 3D tumor spheroids in single-holed hollow particle arrays over the 7-day culture period. The scale bar is 200 μm. (B), (C) and (D) Diameter, area, and roundness change with the extension of incubation time, respectively.

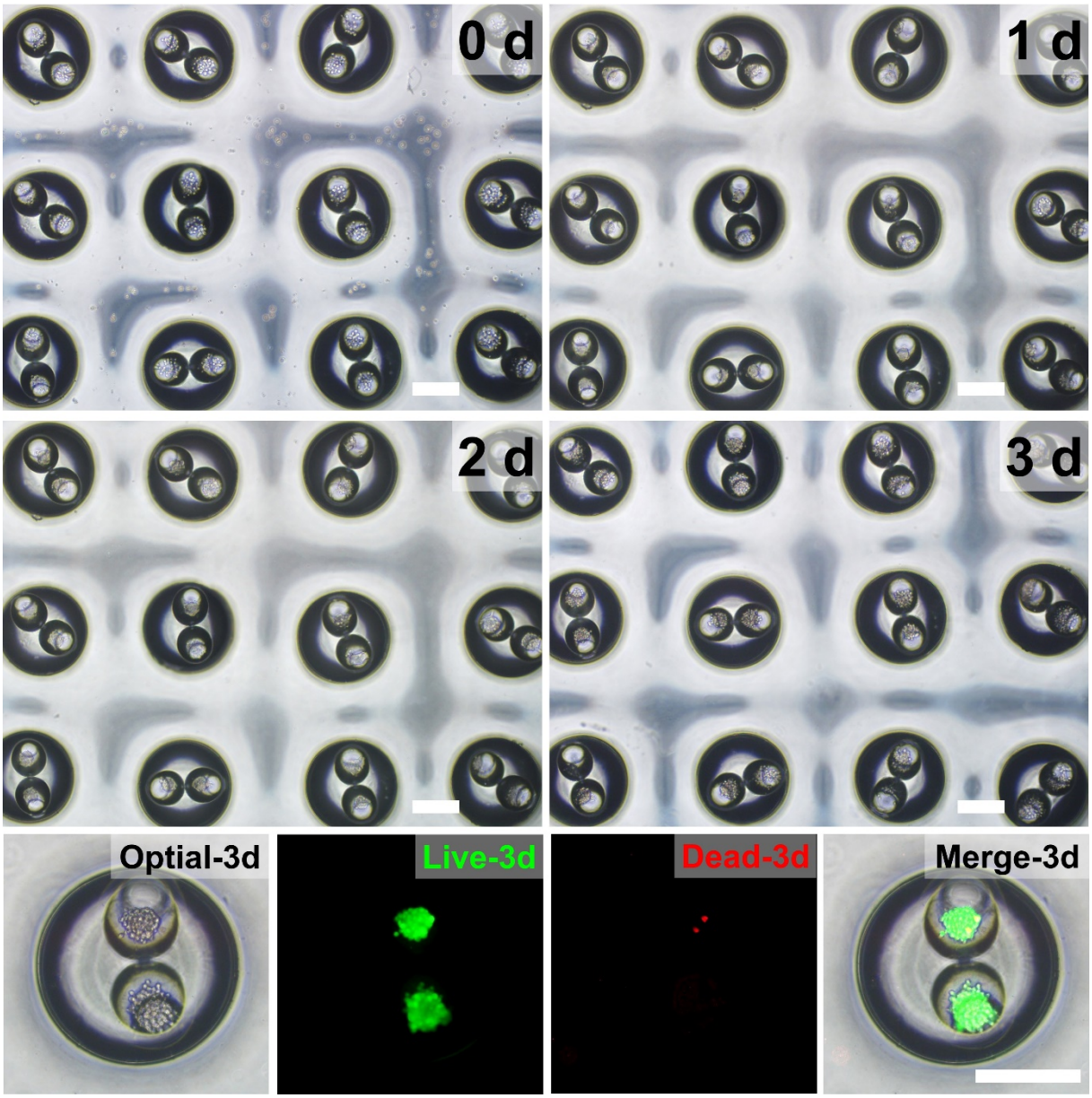

Figure S14. Bright-field images and the corresponding FDA/PI co-staining fluorescent images of HepG2 3D tumor spheroids in double-holed hollow particle arrays over the 3-day culture period. Scale bars are 300 μm.

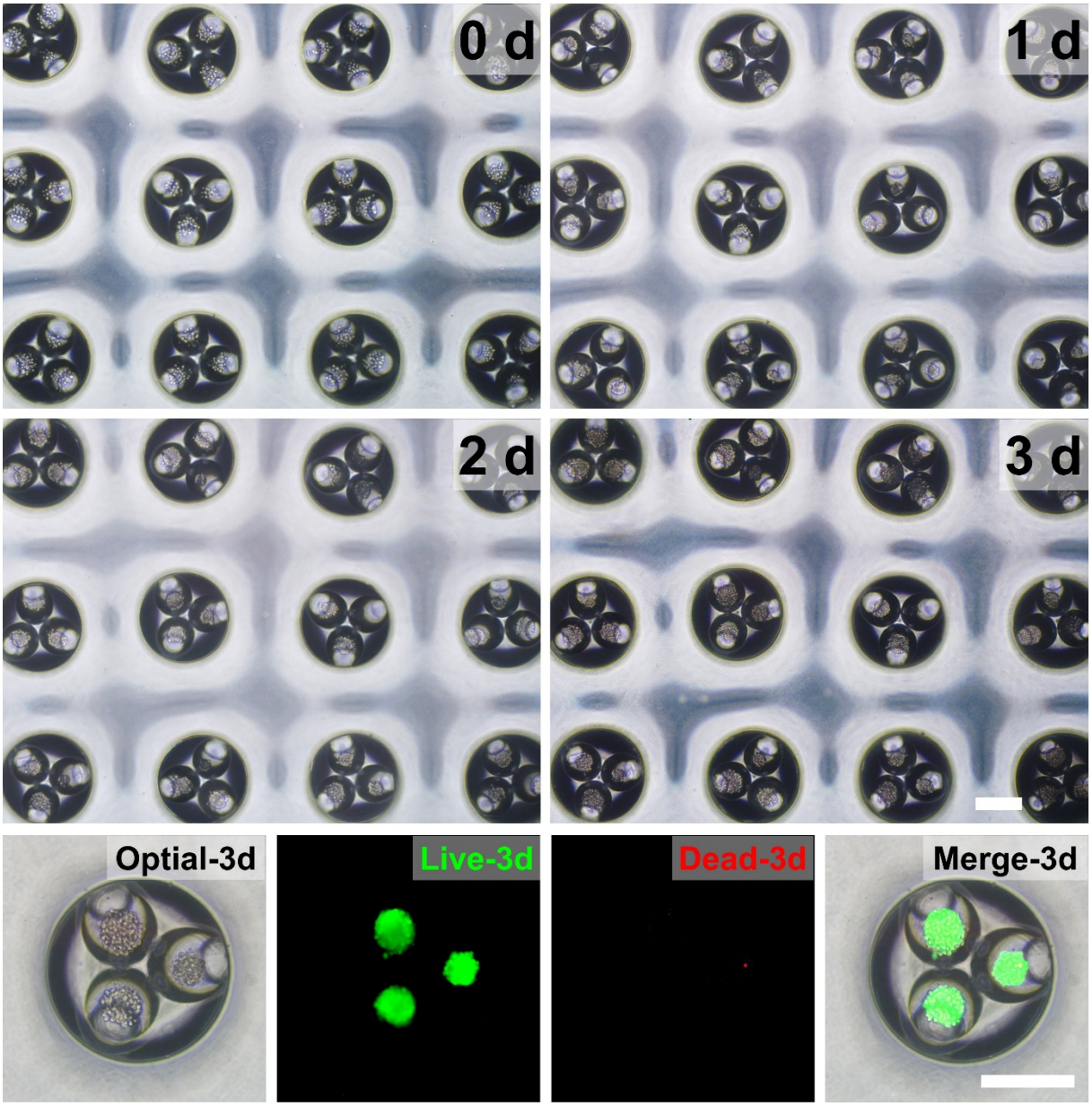

Figure S15. Bright-field images and the corresponding FDA/PI co-staining fluorescent images of HepG2 3D tumor spheroids in triple-holed hollow particle arrays over the 3-day culture period. Scale bars are 300 μm.